# VMAT2 Safeguards β-Cells Against Dopamine Cytotoxicity Under High-Fat Diet–Induced Stress

Daisuke Sakano,[1] Fumiya Uefune,[1] Hiraku Tokuma,[1] Yuki Sonoda,[1] Kumi Matsuura,[2] Naoki Takeda,[3] Naomi Nakagata,[4] Kazuhiko Kume,[5] Nobuaki Shiraki,[1] and Shoen Kume[1]

*Diabetes 2020;69:2377–2391 | https://doi.org/10.2337/db20-0207*

**Vesicular monoamine transporter 2 (VMAT2) uptakes cytoplasmic monoamines into vesicles for storage. VMAT2 plays a role in modulating insulin release by regulating dopamine levels in the pancreas, although the exact mechanism remains elusive. We found that VMAT2 expression in β-cells specifically increases under high blood glucose conditions. The islets isolated from β-cell–specific *Vmat2* knockout (βVmat2KO) mice show elevated insulin secretion levels in response to glucose stimulation. Under prolonged high-fat diet feedings, the βVmat2KO mice exhibit impaired glucose and insulin tolerance and progressive β-cell dysfunction. Here we demonstrate VMAT2 uptake of dopamine to protect dopamine from degradation by monoamine oxidase, thereby safeguarding β-cells from excess reactive oxygen species (ROS) exposure. In the context of high demand for insulin secretion, the absence of VMAT2 leads to elevated ROS in β-cells, which accelerates β-cell dedifferentiation and β-cell loss. Therefore, VMAT2 controls the amount of dopamine in β-cells, thereby protecting pancreatic β-cells from excessive oxidative stress.**

Endocrine pancreatic β-cells are highly specialized for making insulin for the maintenance of glucose homeostasis in our bodies. Diabetes is a disease caused by the lack of (type 1) or dysfunction of (type 2) β-cells. Oversupply of nutrients and the subsequent overstimulation of β-cells contribute to insulin secretory failure in type 2 diabetes. Reactive oxygen species (ROS) are produced from mitochondrial respiration with stimulation with glucose and other fuels. In the pancreatic β-cells, glucose metabolism via the tricarboxylic acid cycle is central for triggering insulin secretion. Higher glucose-stimulated insulin secretion (GSIS) activity triggers more elevated levels of ROS production (1,2). In a healthy state, β-cells possess elaborate antioxidant mechanisms to adapt to the cytotoxicity of ROS. However, chronic overnutrition leads to progressive mitochondrial metabolic dysfunction and oxidative stress. Numerous studies have investigated the mechanisms involved in the progression of β-cell failure, in which ROS play an important role.

There is uptake of monoamines by vesicular monoamine transporter 2 (VMAT2), a protein encoded by the *Slc18a2* gene, from the cytoplasm into the vesicles. Cytoplasmic monoamines, namely, dopamine, serotonin, noradrenaline, adrenaline, and histamine, are transported by VMAT2 into cytosolic vesicles, where they are protected from degradation by monoamine oxidase (MAO) and stored for subsequent release (3–5). Adult β-cells possess the enzymes required to synthesize, interconvert, and catabolize monoamines and to store them in the vesicular granules. Of the two VMAT isoforms that transport monoamines, VMAT2 is the isomer expressed in the pancreas (6–9). Among the monoamines, dopamine is the most abundant monoamine in β-cells (10,11).

During GSIS from pancreatic β-cells, dopamine modulates insulin release. Exogeneous dopamine inhibits GSIS in isolated islets through the Drd2 receptor, which is expressed on β-cells (12). Treatment of rat islets with the VMAT2-specific antagonist tetrabenazine (TBZ) significantly enhanced their

[1]School of Life Science and Technology, Tokyo Institute of Technology, Yokohama, Kanagawa, Japan
[2]Department of Stem Cell Biology, Institute of Molecular Embryology and Genetics, Kumamoto University, Kumamoto, Japan
[3]Division of Developmental Genetics, Institute of Resource Development and Analysis, Kumamoto University, Kumamoto, Japan
[4]Division of Reproductive Engineering, Center for Animal Resources and Development, Kumamoto University, Kumamoto, Japan
[5]Department of Neuropharmacology, Graduate School of Pharmaceutical Sciences, Nagoya City University, Nagoya, Japan

Corresponding authors: Shoen Kume, skume@bio.titech.ac.jp, and Daisuke Sakano, dsakano@bio.titech.ac.jp

Received 2 March 2020 and accepted 17 August 2020

This article contains supplementary material online at https://doi.org/10.2337/figshare.12821411.

insulin secretion (13). Dopamine and its precursor L-dopa inhibit GSIS (14). However, disruption of the dopamine D2 receptor results in impairment of insulin secretion and causes glucose intolerance (15). Furthermore, inhibition of MAO activity reduces insulin secretion in response to metabolic stimuli (16), which raises the possibility that dopamine is important for β-cell function. However, it remains unknown how dopamine affects the function of β-cells.

Previously, we identified TBZ in a screening, searching for small molecular compounds that potentiate the differentiation of embryonic stem (ES) cells into insulin-expressing β-cells (11). We found that treatment with TBZ decreased dopamine content, thereby identifying VMAT2-dopamine signaling as a negative regulator for pancreatic β-cell differentiation. We also identified domperidone, an antagonist for dopamine D2 receptor (Drd2), in another screen as a compound that increases β-cell mass in adult islets (17). We found that the dopamine-Drd2 signal functions as a negative regulator for the maintenance of β-cell mass.

In the current study, to understand the role of VMAT2 and dopamine signaling in the regulation of β-cell and glucose homeostasis, we generated a pancreatic β-cell–specific *Vmat2* mutant mouse line using a rat insulin 2 promotor driving Cre recombinase (RIP-CreER) crossing with a conditional *Vmat2* allele, *Slc18a2*$^{tm1c}$. We found that VMAT2 plays an important role in protecting β-cells from cytotoxicity of ROS.

## RESEARCH DESIGN AND METHODS

### Ethics Approval

All studies involving animals were performed following local guidelines and regulations and were approved by the Institutional Committee for Animal Research in Tokyo Institute of Technology and Kumamoto University.

### Monoamine Content Assay

The monoamine content assay was performed as previously described (11). Isolated islet cells were lysed with lysis buffer containing 1.0% Triton X-100 (Nacalai Tesque, Kyoto, Japan) in 0.1 mol/L PBS (pH 7.2) (Sigma-Aldrich) with protease inhibitor cocktail. Lysates were assayed for dopamine with a dopamine-specific ELISA kit (Labor Diagnostika Nord GmbH & Co. KG, Nordhorn, Germany).

### Generation of Slc18a2$^{tm1a}$, Slc18a2$^{tm1c}$, and Slc18a2$^{tm1d}$ Mouse Lines and a Conditional β-Cell–Specific *Slc18a2* (Vmat2) Knockout Mouse Line, βVmat2KO

An ES cell line bearing a targeted mutation at *Slc18a2* (encoding VMAT2 protein) (*Slc18a2*$^{tm1a(EUCOMM)Wtsi}$; number EPD0242_2_F06) (C57BL/6) was produced for the EUCOMM and EUCOMMTools projects by the Wellcome Trust Sanger Institute. The mutation details (Mouse Genome Informatics [MGI] identifier 4432865) are as follows: The L1L2_Pgk_P cassette was inserted at position 59262507 of chromosome 19 upstream of exon 3 (Build GRCm38). The cassette is composed of an FLP recombinase target (FRT) site followed by En2 SA, IRES and LacZ, SV40 polyA sequences, and a loxP site. This first loxP site is followed by a neomycin resistance (neo) gene under the control of the PGK promoter, SV40 polyA, a second FRT site, and a second loxP site. A third loxP site is inserted downstream of the targeted exon 3 at position 59263523. The exon 3 is thus flanked by loxP sites (Fig. 1). The *tm1a* allele was initially a *Vmat2*-nonexpressing form. Slc18a2$^{tm1a/+}$ mice were generated by injection of the Slc18a2$^{tm1a(EUCOMM)Wtsi}$ ES cells into the perivitelline space of one-cell stage C57BL/6 mouse embryos. We have successfully produced mouse chimeras, 36 males and 15 females, in 200 injections. We then crossed the chimera mice to produce homozygous Slc18a2$^{tm1a/tm1a}$, but all embryos died at embryonic day 11.5. Heterozygous Slc18a2$^{tm1a/+}$ mice were alive and fertile. We then created a "conditional ready" Slc18a2$^{tm1c}$ mouse line (floxed) allele by crossing the Slc18a2$^{tm1a/+}$ mice with a global Flp transgenic mouse strain [Gt(ROSA)26Sortm1(FLP1)Dym/J, stock no. 003946; The Jackson Laboratory, Bar Harbor, ME], so that subsequent cre expression results in a knockout mouse. β-cell–specific *Vmat2* mutant mice were produced by crossing the homozygous Slc18a2$^{tm1c/tm1c}$ with RIP-Cre transgenic mice [B6.Cg-Tg(Ins2-cre)25Mgn/J, stock no. 003573; The Jackson Laboratory]. All mice used were maintained on a C57BL/6 background. PCR primers used for genotyping are listed in Supplementary Table 1.

### SPiDER-βGal Staining of Slc18a2$^{tm1a/+}$ Mouse Islets

Slc18a2$^{tm1a}$ mouse genome bearing the *LacZ* gene was used to report *Vmat2* gene expression (Supplementary Fig. 1). LacZ activity in the Slc18a2$^{tm1a/+}$ pancreas sections was visualized by SPiDER-βGal staining solution (Dojindo Molecular Technologies, Inc., Rockville, MD) (18).

### Measurement of Glucose-Stimulated C-Peptide (Insulin) Secretion by ELISA

For GSIS assays, mouse islets were preincubated for 30 min in low glucose (5.5 mmol/L) in Krebs-Ringer buffer (133.4 mmol/L NaCl, 4.7 mmol/L KCl, 1.2 mmol/L $KH_2PO_4$, 1.2 mmol/L $MgSO_4$, 2.5 mmol/L $CaCl_2$, 5.0 mmol/L $NaHCO_3$, 2.8 mmol/L glucose, 10 mmol/L HEPES [pH 7.4], and 0.2% BSA). Islets were washed twice with PBS and then incubated for 1 h in low glucose (5.5 mmol/L) or high glucose (25.0 mmol/L). Insulin secretion into the buffer and insulin content of the cell lysates were measured using a mouse C-peptide ELISA kit (Shibayagi Co., Ltd., Gunma, Japan) and then normalized with the protein content of the cell lysates.

### High-Fat Diet Feeding

Male mice were housed in a 12-h light-dark cycle. Feedings were switched from normal diet (ND) (AIN-93M; Oriental Yeast Co., Tokyo, Japan) to high-fat diet (HFD) (60% kcal from fat) (HFD-60; Oriental Yeast Co., Tokyo, Japan) at 6 weeks of age.

### Intraperitoneal Glucose Tolerance Test

Mice that had been fasted for 16 h were used. Blood glucose levels were measured before (0 min) and at 15, 30, 60, 90, and 120 min after intraperitoneal administration of 25% glucose solution (Wako, Osaka, Japan) at 1.5 g/kg body wt.

### Intraperitoneal Insulin Tolerance Test

Mice fasted for 6 h were administered with an intraperitoneal injection of insulin solution (0.4 units insulin/kg body wt HUMULIN R [regular human insulin injection]; Eli Lilly, Indianapolis, IN). Glucose levels were monitored.

### Blood Glucose Measurement

Blood glucose levels were measured with OneTouch Ultra equipped with Life Check Sensor (Gunze, Kyoto, Japan) or blood glucose meter ANTSENSE III (Horiba, Kyoto, Japan).

### Insulin Measurements

Blood samples were sampled 30 min after glucose intraperitoneal injection (2 mg/kg) and centrifuged to obtain plasma. Plasma insulin was measured using a Mouse Insulin ELISA Kit (Shibayagi Co., Ltd.).

### F-actin Staining and Immunohistochemistry Analysis

Tissue samples were fixed with 4% formaldehyde, cryoprotected with 30% sucrose, and cut into 10-μm-thick sections. For F-actin staining, Alexa Fluor 555 Phalloidin (cat. no. 8953S, 1:20; Cell Signaling Technology, Tokyo, Japan) was used. For immunohistochemistry, the following antibodies were used: rabbit anti–chromogranin A (ab15160, 1:400; Abcam), mouse anti-glucagon (G2654, 1/1,000; Sigma-Aldrich), guinea pig anti-insulin (A0564, 1/500; Dako), and rabbit anti-VMAT2 (ab81855, 1:500; Abcam). Alexa Fluor 488 donkey anti-guinea pig IgG (706-546-148, 1:1,000; Jackson ImmunoResearch Laboratories, Inc., West Grove, PA), Alexa Fluor 568 donkey anti-rabbit IgG (A10037, 1:1,000; Invitrogen), and Alexa Fluor 647 donkey anti-mouse IgG (Jackson ImmunoResearch Laboratories, Inc.) were used. Tissue sections were counterstained with DAPI (Roche Diagnostics, Basel, Switzerland).

### TUNEL Assay

The TUNEL assay was performed using the In Situ Cell Death Detection Kit, Fluorescein (cat. no. 11684795910; Roche Applied Science, Mannheim, Germany).

### Caspase-3/7 Detection

Caspase-3/7–positive cells were stained with use of the CellEvent Caspase-3/7 Green Detection Reagent (Invitrogen Life Technologies Co., Carlsbad, CA).

### RNA Isolation, cDNA Synthesis, and Real-time PCR

RNA was extracted using the RNeasy Mini Kit (QIAGEN, Hilden, Germany) and then treated with DNase I (QIAGEN). First-strand cDNA was synthesized using a SuperScript VILO cDNA Synthesis Kit (Invitrogen). Real-time PCR analysis was done using THUNDERBIRD SYBR qPCR Mix (Toyobo) with specific primers. All reactions were run on the StepOnePlus Real-Time PCR System (Applied Biosystems). β-Actin was used as an internal control. All primer sequences are listed in Supplementary Table 2.

### Islet Dissociation Culture or Whole Islet Culture

Mouse islets from 13-week-old mutant or control (*Slc18a2*$^{tm1c/tm1c}$) mice were isolated and handpicked as previously described (19). For dissociation culture, islets were incubated with 0.05% trypsin-EDTA (Invitrogen) for 5 min at 37°C, 5% $CO_2$, and pipetted to dissociate into single cells. The dissociated cells were plated in DMEM (glucose concentration: 25 mmol/L) supplemented with 10% FBS, 100 μmol/L nonessential amid acids, 2 mmol/L L-glutamine, 50 units/mL penicillin, 50 μg/mL streptomycin, and 100 μmol/L 2-mercaptoethanol (Sumitomo Bakelite Co. Ltd., Tokyo, Japan). For whole islet culture, isolated islets were used directly for the culture without dissociation.

### ROS Exposure of the Whole Islets

For testing of the vulnerability of whole islets to ROS, $H_2O_2$ was added to the medium and cultured for 6 h and then used for cell count or real-time PCR.

### ROS Staining

Islet cells were plated at a density of 5,000 cells per well in 384-well polystyrene-coated plates. After 24 h, CellROX Green Reagent (Invitrogen) was added to each well at a concentration of 10 μmol/L and mixed vigorously. The fluorescence of CellROX was measured with a plate reader.

### $H_2O_2$ Content Assay

Isolated islet cells were treated with chemical compounds for 1, 6, or 24 h and lysed with lysis buffer containing 3.0% Triton X-100 (Nacalai Tesque) in 0.1 mol/L PBS (pH 7.2) (Sigma-Aldrich) with protease inhibitor cocktail. Lysates were assayed for $H_2O_2$ contents in islet using Amplite Fluorimetric Hydrogen Peroxide Assay Kit (11502; AAT Bioquest, Sunnyvale, CA).

### Chemical Treatments

The dissociated islet cells were seeded on 384-well plates (Sumitomo Bakelite Co. Ltd.) at a concentration at 2,000 cells/well. Next, 0.1 mmol/L TBZ (T284000; Toronto Research Chemicals) and 0.1 mmol/L pargyline (10007852; Cayman Chemical) were added into the medium on day 3. Both compounds were dissolved in DMSO. Therefore, all tests were performed under 0.1% DMSO (v/v) containing condition.

### Statistical Analyses

Data were analyzed by one-way ANOVA and Dunnett multiple comparisons test, except the data for Fig. 5*E*, in which case unpaired Student *t* tests was used. All data are presented as mean ± SD.

### Data and Resource Availability

All data generated or analyzed during this study are included here and in Supplementary Material.

The mutant mouse generated during the current study is deposited in the Mouse Genome Database at the MGI website, The Jackson Laboratory, as Slc18a2<tm1c(EUCOMM)Wtsi> MGI:6386316. The resource will be available from the corresponding author upon reasonable request.

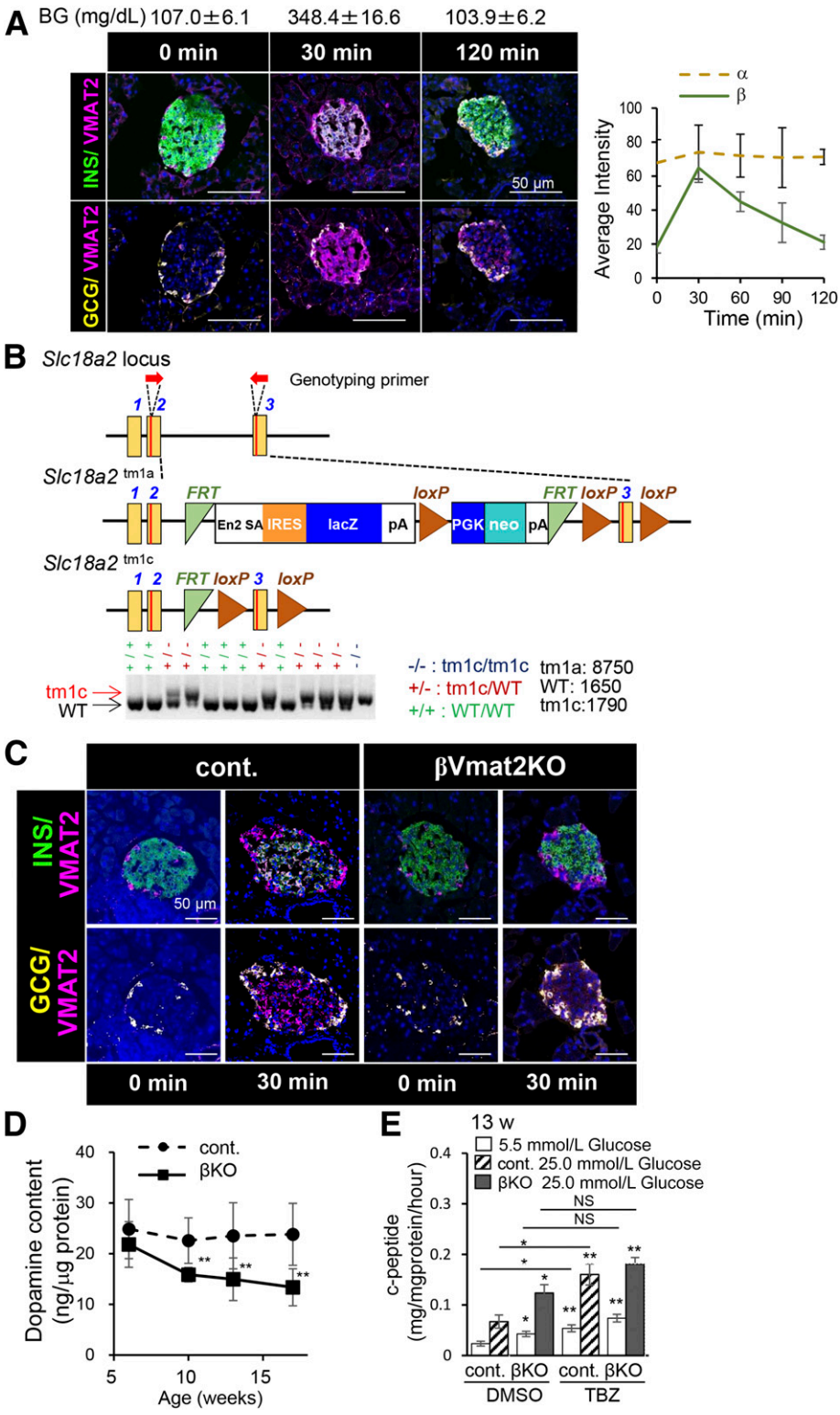


**Figure 1**—VMAT2 expression in the pancreatic islets and the generation of βVmat2KO mouse. *A*: Time-dependent VMAT2 expression in the pancreatic islets in response to glucose administration. Immunostaining of the pancreatic islets (left panel) showed the presence of VMAT2 (magenta) expression in insulin-expressing β-cells under high blood glucose (30 min) but not under low glucose (0 or 120 min) conditions, whereas localization of VMAT2 in glucagon-expressing α-cells was constantly observed. Blood glucose (BG) values of mice at 0, 30, and 120 min are shown above. The average intensity of the VMAT2 protein in β-cells or α-cells was plotted (right panel). *B*: Generation of the *Slc18a2*-deletion mutant mice. The *Slc18a2* locus was inserted with a *LacZ* gene cassette to make the *tm1a* allele (*Slc18a2*$^{tm1a}$). The *tm1c* allele (*Slc18a2*$^{tm1c}$) was obtained by excising the sequence flanked by two FRT sites. βVmat2KO mice were then obtained by crossing homozygous *Slc18a2*$^{tm1c}$ with Ins-Cre transgenic mice. Yellow boxes: exons. Lower panel shows genomic PCR results for genotyping of *Slc18a2*$^{tm1c}$. Genomic PCR products of the *tm1c* or WT *Slc18a2*. *C*: Immunostaining of control and βVmat2KO mouse islets at 10 weeks of age. VMAT2 expression was observed in control (*Slc18a2*$^{tm1c}$) but not the βVmat2KO β-cells, whereas its expression in the α-cells was not

## RESULTS

### β-Cell–Specific Vmat2 Deletion Results in Decreased Dopamine Content and Increased GSIS

Of the two VMAT isoforms that transport monoamines, VMAT1 and VMAT2, VMAT2 is the isoform that is expressed in the β-cells in healthy adult pancreatic islets (6,9). There is debate regarding the cell types that express VMAT2 in rodents (7,8,20). We hypothesized that VMAT2 expression is regulated in a glucose-dependent manner. Therefore, we examined its expression in the mouse pancreatic islets in response to glucose administration. We administered glucose after fasting; then, we monitored blood glucose levels and harvested the pancreas at 0, 30, 60, 90, and 120 min after glucose administration. Immunohistochemistry revealed that VMAT2 expression in the β-cells was regulated in a glucose-dependent manner: VMAT2 expression was downregulated at low blood glucose levels (107 mg/dL) at 0 min, upregulated when blood glucose reached its highest level (348 mg/dL) at 30 min, and subsequently down-regulated with decreasing blood glucose levels at 60, 90, and 120 min after glucose administration. By contrast, VMAT2 was expressed constantly in α-cells in a blood glucose–independent manner (Fig. 1*A*). We used a mouse line, Slc18a2$^{tm1a/+}$, in which a *LacZ* reporter cassette was inserted into Exon3 of the *SLC18a2* gene. We confirmed a similar rapid transient upregulation of *Vmat2* expression, by visualizing LacZ activity using SPiDER-βGal (18), at 30 min after exposure to high glucose (Supplementary Fig. 1). The result suggests that *Vmat2* expression in response to high glucose is, in part, regulated at the transcription level.

To study the function of VMAT2 in β-cells, we created a β-cell–specific VMAT2 mutant mouse line, through the crossing of heterozygous Slc18a2$^{tm1a/+}$ mice with a mouse strain carrying global flp recombinase expression, to produce a "conditional ready" Slc18a2$^{tm1c}$ mouse line (Fig. 1*B*). We then crossed *Slc18a2*$^{tm1c/tm1c}$ with RIP-Cre (21) mice to obtain β-cell–specific *Vmat2* knockout (βVmat2KO) mice (Fig. 1*B*). We confirmed that in the βVmat2KO mice, VMAT2 protein expression in β-cells was nonexistent at high blood glucose levels (30 min after glucose administration), while its expression in the α-cells was equivalent to that in wild-type (WT) mice (Fig. 1*C*).

In pancreatic β-cells, the most abundant monoamine is dopamine (11). We isolated islets from the control (Slc18a2$^{tm1c/tm1c}$) and βVmat2KO mice and measured dopamine content using an ELISA. We found that dopamine content was not affected at 5 weeks but was significantly reduced from 10 weeks, in the βVmat2KO islets compared with the control islets at the same age (Fig. 1*D*).

We then isolated pancreatic islets from 13-week-old mice and examined GSIS and the effect of TBZ, a VMAT2-specific inhibitor, on βVmat2KO islets. βVmat2KO pancreatic islets showed a significantly higher GSIS activity compared with the control islets. We observed potentiation of GSIS by TBZ at low (5.5 mmol/L) and high (25.0 mmol/L) glucose in control, but not in βVmat2KO, islets (Fig. 1*E* [also refer to Fig. 3]).

Our above results confirmed that in the βVmat2KO mice, VMAT2 expression was knocked out specifically in β-cells, which led to a decrease in dopamine content and a higher insulin secretion in response to low or high glucose stimulation.

### Impaired Glucose Tolerance and Insulin Tolerance in HFD-Fed βVmat2KO Mice

To examine the phenotypic changes between the βVmat2KO and the control mice, we first compared body weight and blood glucose levels under ND conditions; however, no significant differences were found (Fig. 2*A* and *B*). We then assayed for glucose tolerance and insulin tolerance and again found no significant differences between the βVmat2KO and control (Slc18a2$^{tm1c/m1c}$) mice (Fig. 2*C* and *E*). It is reported that RIP-Cre mice fed with ND could display glucose intolerance even at 2 months of age in a background of pure C57BL/6 or mixed 129xC57BL/6 background (22), while others reported that no significant glucose intolerance was observed (23). We initially used RIP-Cre$^{+/-}$; Slc18a2$^{tm1c/+}$ heterozygous mice as controls and found that neither glucose intolerance nor insulin intolerance was observed under ND-fed conditions (Supplementary Fig. 2). We then used Slc18a2$^{tm1c/tm1c}$ mice as controls for examining the RIP-Cre$^{+/-}$; Slc18a2$^{tm1c/tm1c}$ homozygous mice in the subsequent experiments.

Since dopamine functions as a negative regulator for β-cell mass (17) and insulin secretion, we hypothesized that impaired VMAT2 function might be critical in conditions of high demand for insulin secretion. We then tested the effects of an HFD on βVmat2KO mice. We started HFD feeding at 5 weeks of age and compared the body weight and blood glucose levels of the mice with those of ND-fed mice. Both control and βVmat2KO mice fed with an HFD showed a rapid increase in body weight and nonfasting blood glucose compared with ND-fed mice (Fig. 2*A* and *B*). We then examined glucose tolerance in these mice. There were no significant differences in glucose tolerance in mice <15 weeks old. However, at 15 weeks of age and onward, HFD-fed βVmat2KO mice exhibited impaired glucose tolerance compared with ND-fed or HFD control mice (Fig. 2*C*). The area under the curve (AUC) of

affected. At the bottom of the panel, 0 or 30 minutes indicates the time after glucose injection. *D*: βVMAT2KO islets showed significantly lower dopamine content compared with that of the control islets. *E*: The effects of TBZ or DMSO treatments on insulin secretion in response to glucose stimulation in the isolated islets. *A* and *C*: VMAT2, magenta; INS, green; GCG, yellow; DAPI, blue. βKO, βVmat2KO. Scale bars = 50 μm. *A*, *D*, and *E*: Means ± SD are shown ($n$ = 3). Significant differences vs. control, by one-way repeated-measures ANOVA and Dunnett multiple comparisons test. cont., control; w, weeks.

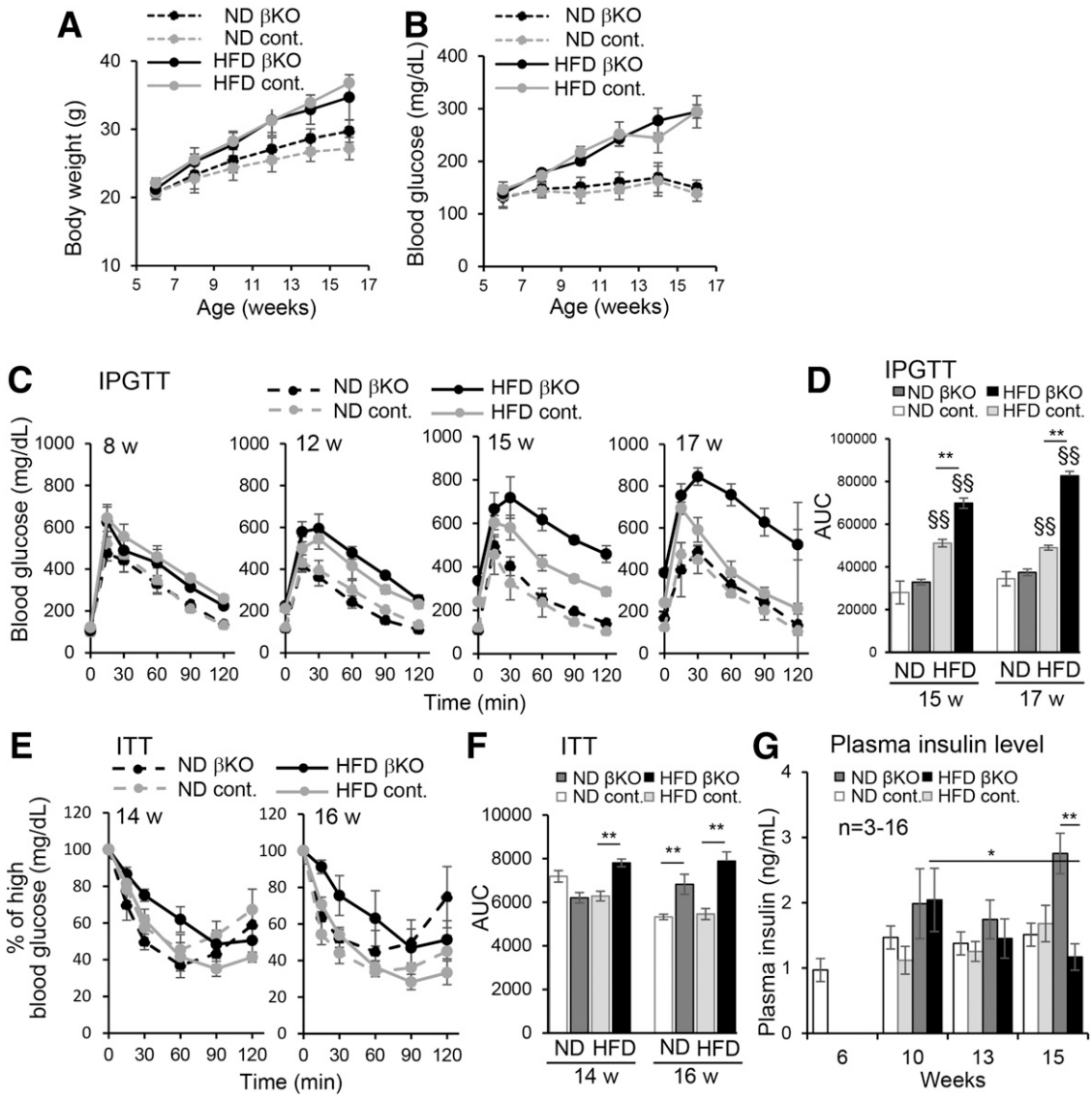


**Figure 2**—βVmat2KO mice exhibited impaired glucose and insulin tolerance after prolonged HFD treatment. *A* and *B*: Age-dependent body weight (*A*) or blood glucose (*B*) of βVmat2KO (βKO) and control (*Slc18a2*$^{tm1c/tm1c}$) mice under ND- or HFD-fed conditions was plotted. No significant difference between the βVmat2KO and control mice was observed under ND- or HFD-fed conditions, respectively. Body weight and blood glucose were elevated in the HFD-fed groups. *C*: Intraperitoneal glucose tolerance tests (IPGTTs) were performed in 8-, 12-, 15-, and 17-week-old βVmat2KO and control mice. The time dependence of blood glucose levels after glucose administration is shown. βVmat2KO but not control mice showed impaired glucose tolerance at 15 weeks and 17 weeks of age. *D*: AUC of the results at 15 weeks and 17 weeks shown in *C* reveals that HFD-fed βVmat2KO mice show impaired glucose tolerance compared with that of the ND-fed control mice. *E*: Insulin tolerance tests (ITTs) were performed with 14- and 16-week-old βVmat2KO and control mice. Plasma glucose levels were presented as % change from glucose level at time 0. *F*: AUC of the results shown in *E* reveals that HFD-fed βVmat2KO mice at 14 weeks or 16 weeks of age showed impaired insulin tolerance compared with that of the HFD-fed control mice of the same age (**$P < 0.01$). *G*: The plasma insulin levels of 13-, 15-, and 17-week-old mice were calculated. The results of βVmat2KO fed with ND or HFD were compared with those of control mice. The result of the control mouse at 6 weeks is displayed for comparison. Means ± SD are shown. ($n = 5$–10); significant differences vs. ND-fed control, §$P < 0.05$ and §§$P < 0.01$, or significant differences between two values marked by the bars, *$P < 0.05$ and **$P < 0.01$, by one-way ANOVA and Dunnett multiple comparisons test. cont., control; w, weeks.

blood glucose concentration following glucose stimulation in 15- and 17-week-old HFD-fed βVmat2KO or control mice was significantly increased compared with that of the ND-fed control mice, with the AUC of the HFD-fed βVmat2KO even higher than that for control mice (Fig. 2*D*). The results indicate that HFD-fed βVmat2KO mice developed impaired glucose tolerance at increasing ages (>15 weeks). We then assessed the insulin tolerance of the mice at 14 and 16 weeks of age and found that βVmat2KO mice exhibited impaired insulin tolerance compared with ND-fed or HFD control mice (Fig. 2*E*). The AUC in HFD-fed βVmat2KO mice was significantly increased in 14- and

16-week-old mice (fed with HFD for 8 and 10 weeks, respectively) compared with that of the control mice (Fig. 2*F*). It was reported that C57BL/6 mice developed insulin resistance after > 11 weeks of HFD feeding (24). Our results show that HFD-fed βVmat2KO mice developed insulin intolerance before the control mice became overtly insulin intolerant. Our results demonstrate that prolonged HFD feeding led to impaired glucose tolerance and deteriorated insulin tolerance in βVmat2KO mice. We then measured plasma insulin levels. Plasma insulin gradually decreased in HFD-fed βVmat2KO but not in control mice. The result suggests that the impaired glucose tolerance observed in the HFD-fed βVmat2KO mice is due to the reduced plasma insulin level.

### Pancreatic Islets of HFD-Fed βVmat2KO Mice Showed an Initial Increase in β-Cell Mass Followed by Impaired GSIS and β-Cell Loss With Increasing Age

To investigate the underlying molecular mechanism that triggers β-cell dysfunction in HFD-fed βVmat2KO mice, we performed an immunohistochemical analysis of the pancreatic islets harvested from mice at 30 min after glucose administration. A lack of VMAT2 expression was confirmed in the βVmat2KO β-cells but not the control β-cells under high blood glucose conditions, while expression of insulin and glucagon was not affected (Fig. 3*A* and *B*). We observed an increase in β-cell mass in young mice at 10 and 13 weeks of age in both βVmat2KO and control HFD-fed mice compared with ND-fed mice (Fig. 3*A* and *B*). The enlarged islets were present in control mice fed with an HFD throughout observation (up to 17 weeks of age) (Fig. 3*B*). In contrast, the β-cell mass decreased in HFD-fed βVmat2KO mice at 15 weeks of age and became much smaller at 17 weeks (Fig. 3*A* and *B*). The above results were confirmed by quantitative analysis of β-cell mass and islet mean size (Fig. 3*C* and *D*). On the other hand, the *Vmat2* expression levels were not significantly different between ND- and HFD-fed control islets at all ages (Fig. 3*E*).

We then isolated pancreatic islets from ND- and HFD-fed βVmat2KO and control mice and performed GSIS analysis in vitro. The islets of ND-fed βVmat2KO mice exhibited significantly elevated levels of insulin secretion compared with the control mice at all ages examined, in agreement with the above results (Fig. 1*E*). With HFD feeding, islets isolated from control mice showed elevated GSIS activity. In contrast, islets isolated from HFD-fed βVmat2KO mice showed elevated GSIS at 10 weeks of age, but GSIS activity decreased at 13 and 15 weeks of age in spite of the large β-cell mass at 13 weeks, suggesting that β-cell dysfunction occurred (Fig. 3*F*).

These results suggest that the pancreatic islets of βVmat2KO mice secrete an elevated level of insulin even under low glucose conditions and respond to high glucose by secreting a higher level of insulin compared with the control mice. βVmat2KO β-cells can meet the metabolic requirements of mice and maintain blood glucose homeostasis under ND conditions. Under HFD conditions, a compensatory increase in β-cell mass occurred in control mice to meet the increased metabolic demands. However, in the βVmat2KO mice, β-cells could not overcome the increased metabolic demands, resulting in β-cell dysfunction and eventual β-cell loss.

### Dedifferentiation of β-Cells Is Accelerated in HFD-Fed βVmat2KO Islets

β-cell dedifferentiation is known as a mechanism that underlies β-cell dysfunction in type 2 diabetes (25). We found that HFD feeding triggered insulin resistance in βVmat2KO mice. Therefore, we investigated the possibility that dedifferentiation might contribute to β-cell dysfunction by evaluating the expression of chromogranin A (CGA), whose expression is lost upon β-cell failure (26). We detected CGA expression in all ages of β-cells. While CGA expression was reduced in HFD-fed control β-cells at 15 weeks of age, CGA expression almost disappeared in HFD-fed βVmat2KO β-cells (Fig. 4*A* and *B*). Since actin remodeling functions during insulin secretion (27), we examined fiber-like F-actin and found a loss of F-actin (Fig. 4*C* and *D*) from the islets of HFD-fed βVmat2KO mice but not the islets of control mice at 15 weeks of age. We then examined the expression of other differentiation markers by real-time PCR in islets from ND- or HFD-fed control or βVmat2KO mice. To allow comparison across genotypes, we show expression levels as relative values versus those of ND-fed controls. It was reported that a reduction in the expression of differentiation markers was observed after HFD feeding for 12 weeks or 16 weeks (24). Here, even at early periods when expressions of most β-cell maturation markers were not yet observed in the HFD-fed control islets, decreased expression levels of *Ins1*, *Ins2*, *Nkx6*.1, *Pdx1*, *Glut2*, *Glucokinase* (*Gck*), and *MafA* were observed in the HFD-fed βVmat2KO mice. On the other hand, increased expression of *MafB* and *Aldh1a3* was observed in the HFD-fed βVmat2KO and control islets at 13 or 15 weeks of age (HFD feeding for 7–9 weeks) (Fig. 4*E*), whereas no change in the expression of endocrine progenitor marker *Neurog3* was observed (Fig. 4*E*). Our results revealed that accelerated dedifferentiation seemed to occur in the β-cells of HFD-fed βVmat2KO mice compared with the ND-fed control, which led to β-cell loss and β-cell dysfunction.

We then examined cell proliferation and β-cell death. The expression levels of cell cycle regulator genes, cyclin D1 (*CcnD1*), cyclin D2 (*CcnD2*), and proliferating cell nuclear antigen (*Pcna*), were upregulated in HFD-fed control and βVmat2KO islets from 10 or 13 weeks of age (HFD feeding for 4 or 7 weeks). However, their expression levels decreased at 15 weeks of age in HFD-fed βVmat2KO mice (Fig. 5*A*). Concurrently, TUNEL-positive cells increased significantly in the HFD-fed βVmat2KO mice (Fig. 5*B–D*).

Our results confirmed that HFD triggered the dedifferentiation and adaptive proliferation of β-cells, as previously reported (24,28,29). In HFD-fed βVmat2KO islets,

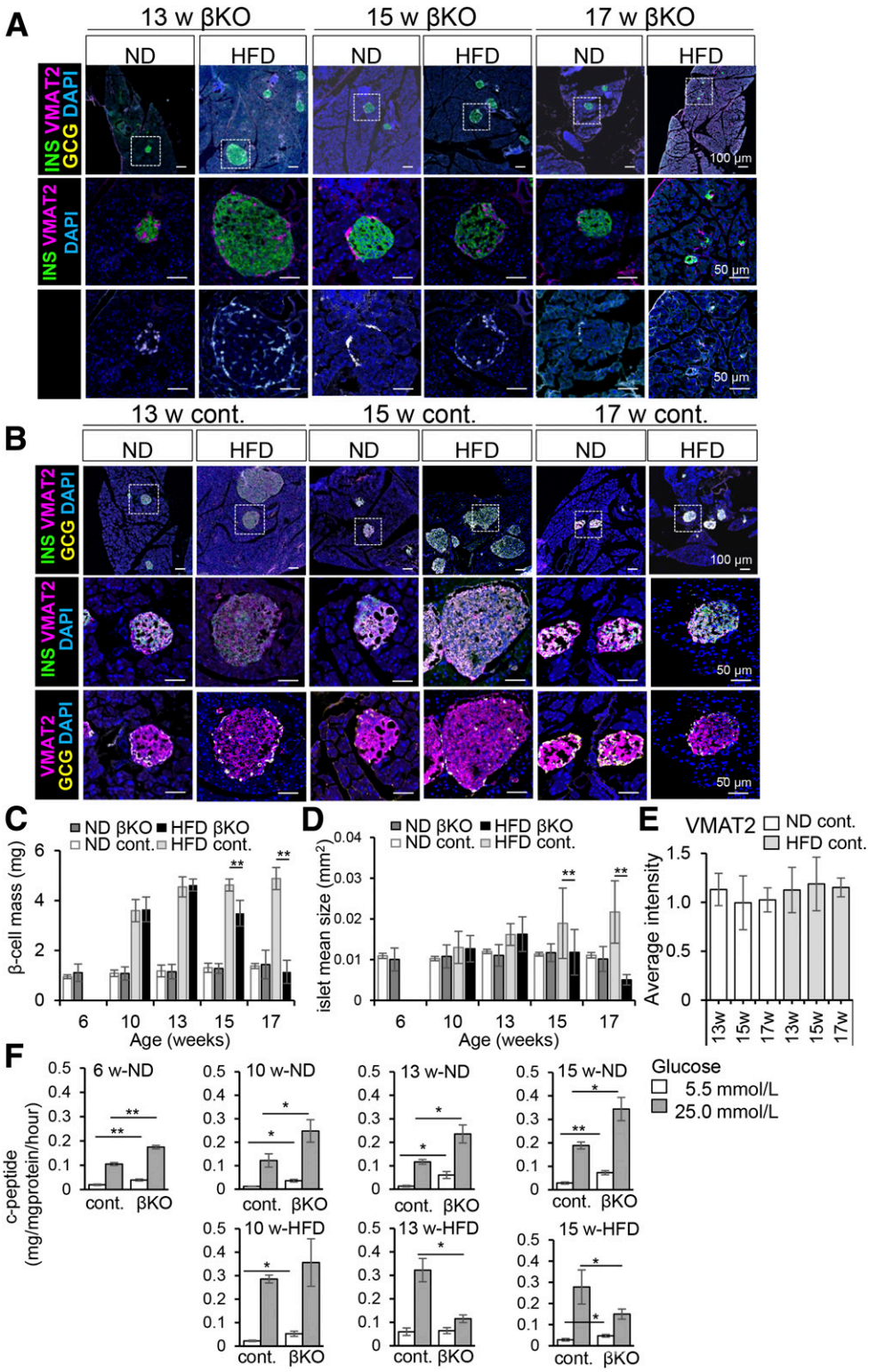


**Figure 3**—HFD-fed βVmat2KO islets showed initial β-cell mass increase followed by β-cell loss. *A* and *B*: Immunostaining of βVmat2KO (βKO) (*A*) and control (*Slc18a2*$^{tm1c/tm1c}$) (*B*) islets under ND- or HFD-fed conditions at 13 weeks, 15 weeks, and 17 weeks of age. In βVmat2KO islets, VMAT2 protein expression was not observed in β-cells but remained in α-cells. At 13 weeks of age, β-cell mass in HFD-fed βVmat2KO and control islets increased. At 15 weeks of age, β-cell mass in HFD-fed βVmat2KO but not control mice began to decrease, and β-cell mass further decreased at 17 weeks of age. VMAT2, red; INS, green; GCG, yellow. Scale bars = top panels, 100 μm; middle and lower panels, 50 μm. *C* and *D*: Quantitative analysis of the age-dependent changes in β-cell mass (*C*) and islet mean size (*D*) in the βVmat2KO and control mice fed with ND or HFD. *E*: Quantitative analysis of the intensity of anti-VMAT2 antibody staining shown in *B*. *F*: Isolated islets from ND- or HFD-fed mice at 6 weeks, 10 weeks, 13 weeks, or 15 weeks old were assayed for insulin secretion in response to glucose stimulation. *C*–*F*: Means ± SD are shown ($n = 3$); significant differences between two values marked by the bars, $^*P < 0.05$ and $^{**}P < 0.01$, by one-way ANOVA and Dunnett multiple comparisons test. cont., control; w, weeks.

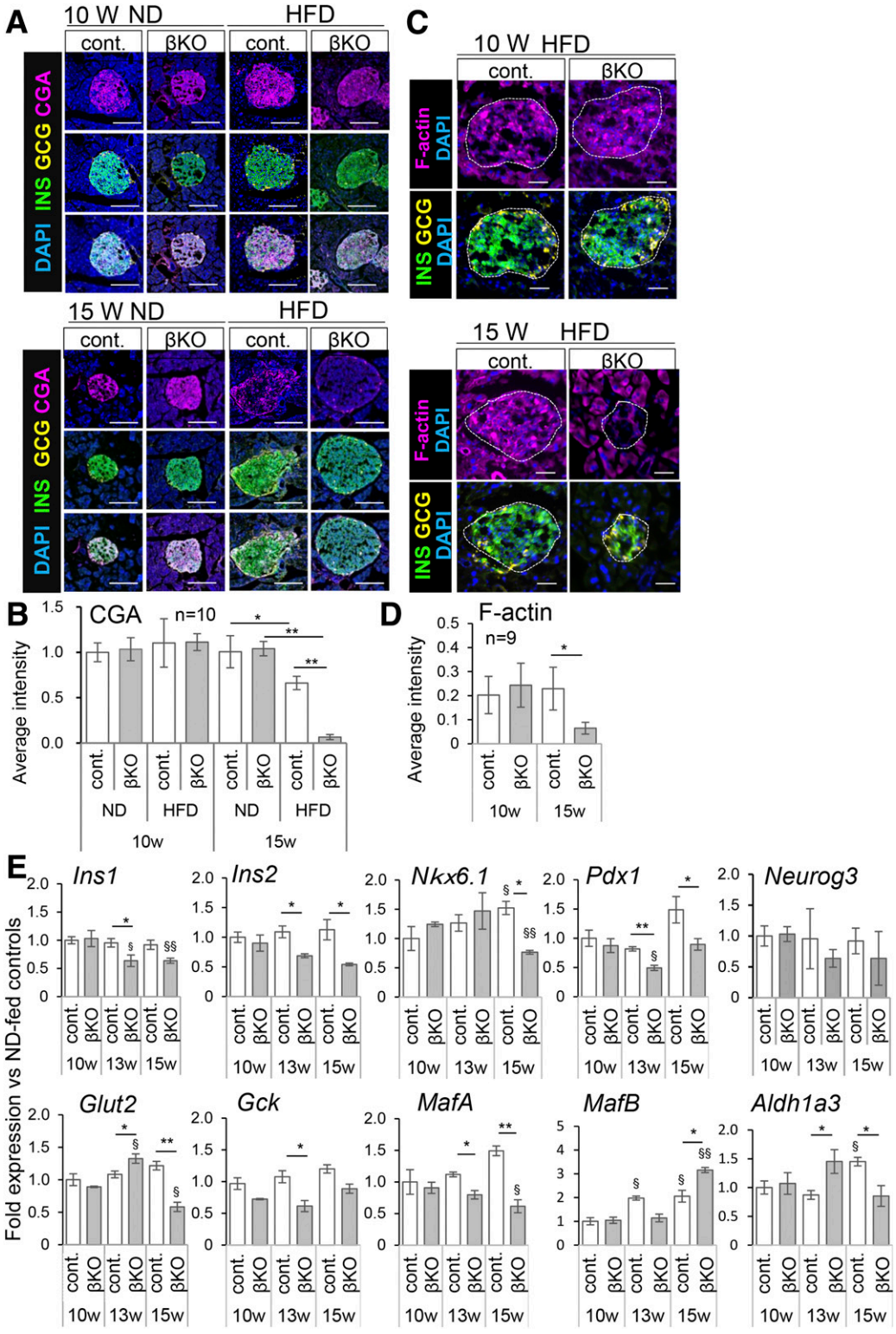


**Figure 4—**Dedifferentiation of β-cells occurs in βVmat2KO mouse islets. *A–D*: Immunostaining of ND- or HFD-fed βVmat2KO (βKO) and control *Slc18a2*$^{tm1c}$ islets isolated at 10 weeks (upper panels) and 15 weeks (lower panels) of age for CGA (magenta) (*A* and *B*) or F-actin (magenta) (*C* and *D*) is shown. *B* and *D*: Quantitative analyses of CGA (*B*) or F-actin (*D*) staining are shown. In 15-week-old βVmat2KO islets, CGA and F-actin staining in β-cells decreased. INS, green; GCG, yellow. Sections were counterstained with DAPI (blue). Scale bars = 50 μm. *E*: Real-time PCR analyses of age-dependent expression of endocrine maturation markers at 10 weeks, 13 weeks, and 15 weeks of age. The values of the HFD-fed WT or βVmat2KO mice are shown as fold expression vs. ND-fed control or βVmat2KO, respectively. *B*, *D*, *E*: Means ± SD are shown ($n = 3$); significant differences between βVmat2KO mice and their 10-week-old controls, §$P < 0.05$ and §§$P < 0.01$, or between two values marked by the bars, *$P < 0.05$ and **$P < 0.01$, by one-way ANOVA and Dunnett multiple comparisons test. Control, white bars; βVmat2KO, gray bars. cont., control; W, weeks.

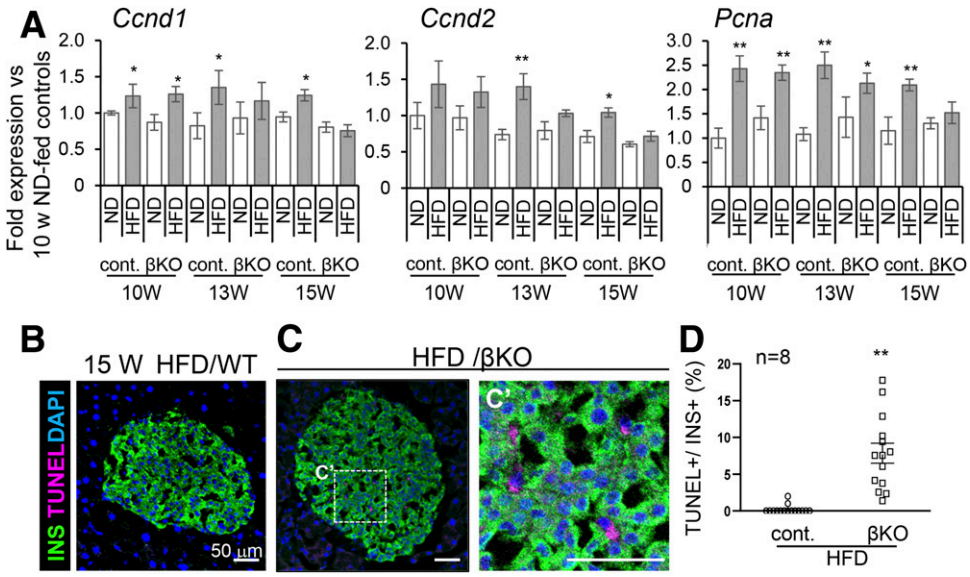


**Figure 5**—β-cell–specific *Vmat2* deletion increased the expression levels of cell-cycle regulator genes and induced apoptosis under HFD-fed conditions. *A*: Expression levels of *Ccnd1*, *Ccnd2,* and *Pcna* in the HFD-fed control *Slc18a2*$^{tm1c}$ or βVmat2KO islets. Values are shown as fold expression vs. in 10-week-old ND-fed control mice. Means ± SD are shown ($n = 3$); significant differences between βVmat2KO and control, $^{*}P < 0.05$ and $^{**}P < 0.01$, by one-way ANOVA and Dunnett multiple comparisons test. *B–D*: TUNEL staining followed by immunostaining of the pancreas tissue sections from HFD-fed control (*B*) or βVmat2KO (*C*) mice. C': High magnification of the box shown in *C*. TUNEL, magenta; INS, green; DAPI, blue. Scale bars = 50 μm. *D*: The proportion of TUNEL-positive cells within insulin-expressing β-cells. Scattered plots with individual results together with mean ± SD are presented. Significant differences were analyzed by unpaired two-tailed Student *t* test and are shown as $^{**}P < 0.01$. $N = 8$. βKO, βVmat2KO; cont., control; W, weeks.

dedifferentiation and cell death in β-cells are accelerated compared with in controls, which seems to attribute to β-cell failure.

### βVmat2KO β-Cells Are Exposed to Elevated ROS Due to Cytoplasmic Dopamine Degradation and Are More Vulnerable to ROS-Induced Cytotoxicity

We then attempted to reveal the underlying molecular mechanism that triggers the dedifferentiation of β-cells in the islets of βVmat2KO mice. The dopamine content in the islets of βVmat2KO mice decreased with age (Fig. 1*D*). The reduction in dopamine content was attributed to the MAO-mediated cytoplasmic degradation of dopamine, which contributes to ROS production through $H_2O_2$ synthesis during substrate degradation (30).

We hypothesized that ROS production in the islets of βVmat2KO mice is higher, as VMAT2 depletion leads to increased cytoplasmic dopamine. To test our hypothesis, we used an islet dissociation culture system (Fig. 6*A–D*), in which islets from ND-fed control or βVmat2KO mice were cultured in vitro. We visualized the production of ROS using a fluorogenic probe. We observed a significantly higher ROS intensity in the β-cells of βVmat2KO mice compared with controls (Fig. 6*A* and *B*). TBZ treatment increased ROS intensity in control but not βVmat2KO islets, and treatment with pargyline, an MAO inhibitor, reversed the increase in ROS. The number of β-cells in control islets was reduced by TBZ treatment (Fig. 6*C*). β-cell apoptosis (activated caspase-3/7+ within Ins+ cells) increased in high glucose conditions and under TBZ treatment and was rescued by pargyline treatment (Fig. 6*D*).

We then used a whole islet culture system and measured the time-dependent generation of $H_2O_2$ by glucose stimulation using islets isolated from ND-fed control or βVmat2KO mice (Fig. 6*E*). In control islets, high glucose stimulation alone showed a slight increase in $H_2O_2$ level in whole islet culture. High glucose alone elevated ROS production (Fig. 6*E* [compare left and middle panels]), which is reported to be toxic in β-cells (31,32). However, in the presence of TBZ, high glucose stimulation induced a rapid and dramatic elevation in $H_2O_2$ levels, which decreased with time and returned to basal levels after 24 h and was rescued by the addition of pargyline (Fig. 6*E*, left and middle panels). In the islets of βVmat2KO mice, the $H_2O_2$ level was highest at 1 h after glucose stimulation without TBZ treatment. Pargyline treatment significantly lowered the $H_2O_2$ level in the islets of βVmat2KO mice (Fig. 6*E*, right panel). It has been reported that exogenous $H_2O_2$ treatment under basal glucose concentrations induced ROS generation up to a similar level with high glucose stimulation (33). We then examined β-cell number after exposure of the islets to different $H_2O_2$ concentrations and found that the islets of βVmat2KO had a significantly lower number of living β-cells than the control mice (Fig. 6*F*). The results suggested that βVmat2KO islets are more sensitive to ROS.

It is reported that β-cells possess antioxidant mechanisms, such as the induction of the transcription factor nuclear factor erythroid 2p45-related factor 2 (*Nrf2*), which

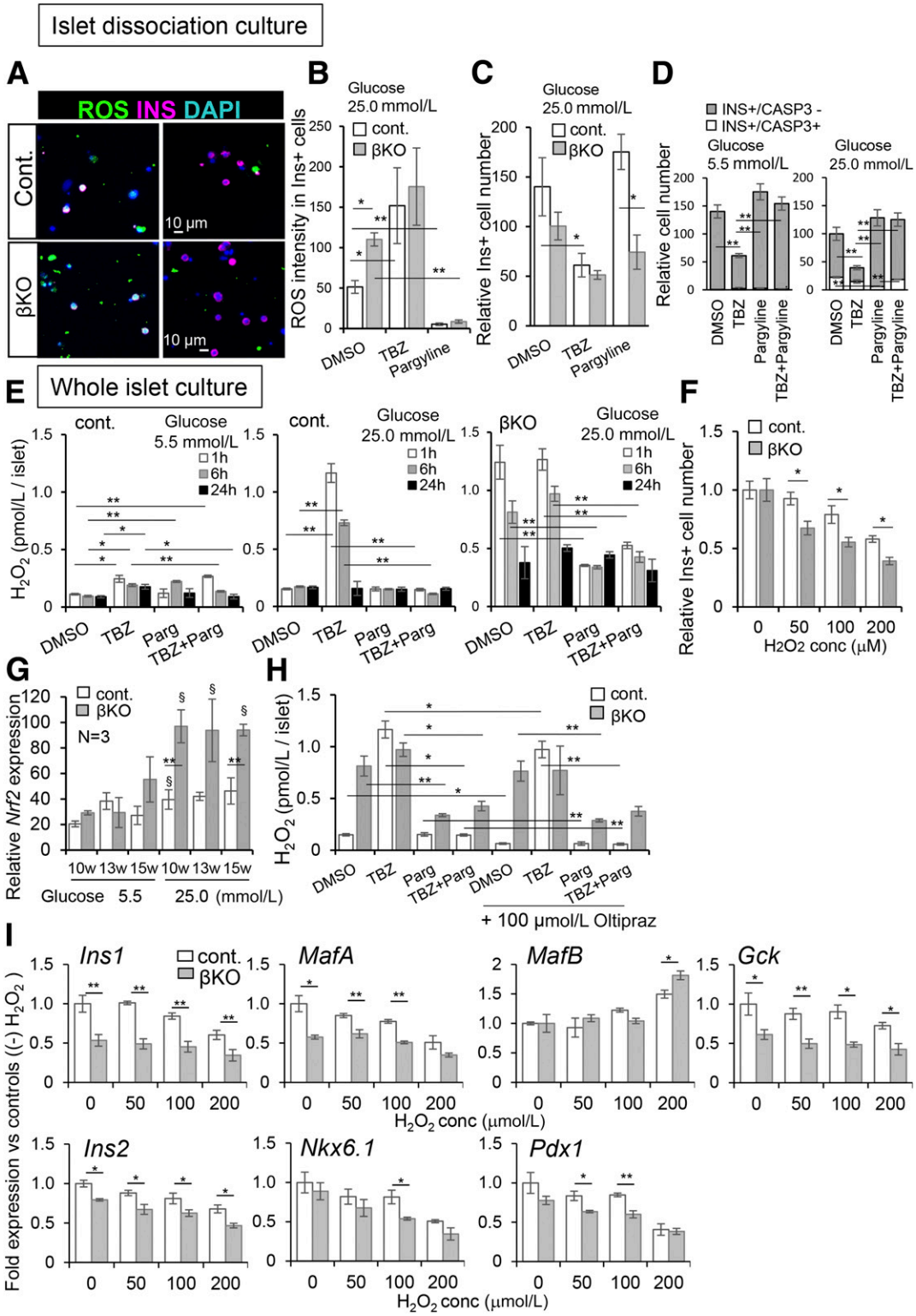


**Figure 6—**ROS level is significantly higher in βVmat2KO compared with control mouse islets, which confer the vulnerability of βVmat2KO. *A–D*: Islet dissociation culture. Images (*A*) and quantification (*B*) of ROS staining in dissociated islets cultured on day 5 under high glucose conditions (25 mmol/L glucose). Compared with control (*Slc18a2*$^{tm1c/tm1c}$) islets, βVmat2KO isolated islets showed a higher ROS level, and both were reduced by treatment with 1 μmol/L pargyline, an MAOB inhibitor. Mice at 13 weeks of age were used. ROS, green; INS, magenta; DAPI, blue. *C* and *D*: Control or βVmat2KO β-cell numbers treated with chemicals or DMSO were quantified after 5 days of dissociation cultures. The number of β-cells in control islets was reduced by TBZ treatment. *D*: The proportion of β-cells that underwent apoptosis (caspase-3/7+) increased under high glucose conditions and was reduced by pargyline treatment, but this was reversed by TBZ + pargyline. CASP3, caspase-3/7. *E–H*: Whole islet culture. *E*: $H_2O_2$ generation under low glucose (5.5 mmol/L [left panel]) or high glucose (25.0 mmol/L [middle panels]) conditions in the isolated islets from ND-fed control (left and middle panels) or βVmat2KO (right panel) mice, treated with chemicals. $H_2O_2$ was quantified at 1 h, 6 h, and 24 h after high glucose (25.0 mmol/L) stimulation. *F*: β-cell number in βVmat2KO or control

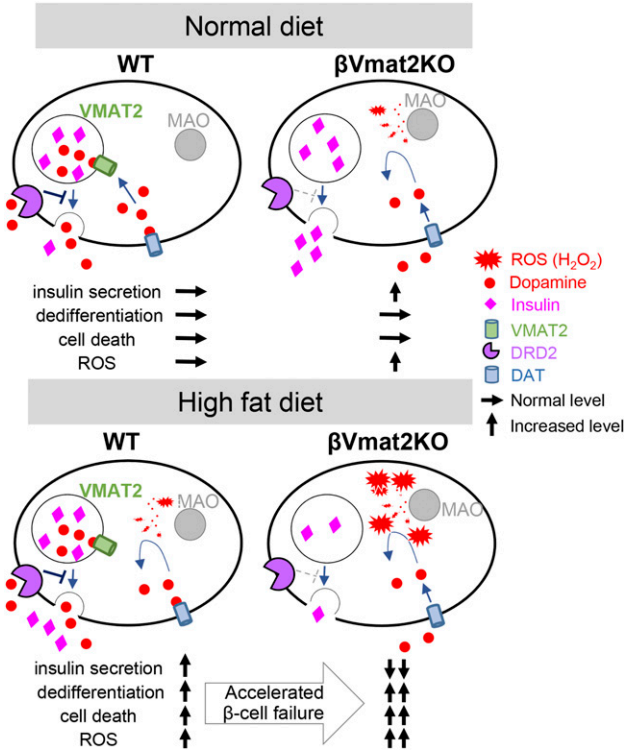


**Figure 7**—Schematic drawing of the molecular mechanism by which VMAT2 safeguards β-cell function under HFD from dopamine-mediated cytotoxicity. Dopamine is released at insulin secretion following high glucose stimulation and acts as a negative regulator for insulin secretion through dopamine receptor 2 (Drd2). Dopamine is normally taken up through dopamine transporter (DAT) and stored in VMAT2-regulated vesicles. Under ND, βVMAT2KO β-cells exhibit increased insulin release in response to glucose stimulation. Under HFD, where insulin secretion occurs frequently, β-cells are under long-term exposure to ROS and become vulnerable to damages by dopamine cytotoxicity, leading to accelerated dedifferentiation and cell death. Left, control *Slc18a2*$^{tm1c/tm1c}$; right, βVMAT2KO β-cells.

regulates the expression of several genes involved in redox metabolism (34). *Nrf2* expression significantly increased in response to high glucose stimulation, to a greater extent in βVmat2KO islets compared with the control mice (Fig. 6*G*). The result suggests that βVmat2KO mice are exposed continuously to high ROS and therefore develop a protective mechanism in response to high glucose stimulation.

Since ROS are mainly produced during mitochondrial respiration, we then assessed the proportion of MAO-mediated ROS generation, by treating islets with oltipraz, an antioxidant that exerts mitochondrial protective effects in β-cells (35). We found that approximately one-half of the $H_2O_2$ generated was reduced by oltipraz treatment in control islets (Fig. 6*H*). Pargyline treatment decreased ~92% of the $H_2O_2$ produced by TBZ. Oltipraz treatment of the TBZ + pargyline islets further reduced the remaining <8% of the $H_2O_2$ triggered by TBZ. Similarly, oltipraz treatment did not reduce $H_2O_2$ in βVmat2KO islets. By contrast, pargyline treatment significantly reduced $H_2O_2$ in βVmat2KO islets. Therefore, our results suggest that a large proportion of ROS generated upon TBZ treatment or in βVmat2KO islets was derived from MAO-mediated generation of ROS, which plays a vital role in the progression of β-cell failure in these models.

Real-time PCR analysis of the $H_2O_2$-treated islets revealed that the islets of βVmat2KO mice expressed mature markers such as *Ins1*, *Ins2*, *MafA*, *Nkx6.1*, *Gck*, and *Pdx1* at significantly lower levels and expressed an immature marker, *MafB*, at significantly higher levels compared with control mice in response to $H_2O_2$ (Fig. 6*I*).

Therefore, we infer that high glucose triggers dopamine secretion and insulin secretion simultaneously. In the presence of VMAT2, cytoplasmic dopamine is rapidly sequestered and stored. However, in the absence of VMAT2 function, cytoplasmic dopamine cannot be sequestered, and dopamine degradation by MAO results in rapid production of $H_2O_2$ upon high glucose stimulation. βVmat2KO β-cells show elevated insulin secretion even under low glucose conditions. β-cells are exposed continuously to ROS. They then develop antioxidative mechanisms to protect themselves. However, being placed under chronic exposure to ROS, βVmat2KO islets are more vulnerable to $H_2O_2$ toxicity than those of the controls. Under prolonged HFD feeding, where a high metabolic demand occurs, dedifferentiation, β-cell dysfunction, and β-cell loss are trigged in βVmat2KO β-cells.

## DISCUSSION

Pancreatic β-cells are susceptible to oxidative stress. Oversupply of nutrients, such as glucose and fatty acids, and overstimulation of β-cells are considered to contribute to β-cell failure in type 2 diabetes. Here, we found that VMAT2 acts to protect β-cells from the toxic effects of oxidative stress triggered by excessive insulin secretion through the compartmentalization of dopamine, which prevents its degradation. VMAT2 protein expression is regulated in a glucose-dependent manner so that β-cells in high glucose conditions show an upregulated VMAT2

islets after $H_2O_2$ treatment. $H_2O_2$ decreased βVmat2KO β-cell number compared with untreated control. *G*: Real-time PCR analyses of *Nrf2* expression in whole islet culture treated with 5.5 or 25.0 mmol/L glucose at 10 weeks, 13 weeks, and 15 weeks of age. *H*: $H_2O_2$ contents in whole islets treated with chemicals, with or without cotreatment of 100 μmol/L oltiplaz for 6 h. *I*: A decrease in the expression of endocrine maturation markers by exposure to $H_2O_2$ in βVmat2KO islets compared with control from ND-fed isolated islets at 13 weeks of age. Values are shown as fold expression vs. controls. Means ± SD are shown ($n = 3$) (*B–I*). Control, white bars; βVmat2KO, gray bars. Significant differences vs. 10-week-old controls, §$P < 0.05$ and §§$P < 0.01$, or between two values marked by the bars, *$P < 0.05$ and **$P < 0.01$, by one-way ANOVA and Dunnett multiple comparisons test. βKO, βVmat2KO; conc, concentration; cont., control; Parg, pargyline; w, weeks.

expression. It is reported that there are tyrosine hydroxylase activities in the adult rat islets themselves (36). Therefore, β-cells synthesize dopamine themselves and store it in the vesicle via VMAT2 to prevent degradation by MAO. Upon insulin secretion in response to high glucose in normal control β-cells, dopamine is secreted into the extracellular space through exocytosis and acts as negative feedback for insulin secretion through binding to its receptor Drd2, which exists on the β-cell plasma membrane. Extracellular dopamine is cleared by reuptake into the β-cells through dopamine plasma membrane transporter DAT and stored in the vesicle via VMAT2 for subsequent release (Fig. 7). In this way, VMAT2 plays a significant regulatory role in the compartmentalization of dopamine. βVmat2KO β-cells (or control β-cells treated with VMAT2 inhibitor TBZ) cannot uptake dopamine into vesicles; thus, dopamine is subjected to degradation by MAO, leading to a reduced dopamine content and an increased generation of ROS. The decreased dopamine content leads to a reduction in the dopamine negative-feedback loop, which in turn leads to elevated insulin secretion. Under HFD conditions, where excess nutrient stress exists, insulin secretion frequently occurs, increasing β-cell exposure to ROS. In βVmat2KO β-cells, HFD triggers chronic exposure to MAO-derived ROS and leads to increased vulnerability and accelerated β-cell failure. βVmat2KO β-cells show an initial compensation via β-cell growth and increased β-cell mass followed by dedifferentiation and β-cell death, which is a characteristic of the progression of β-cell failure (Fig. 7).

### Dedifferentiation Is the Mechanism of β-Cell Failure

HFD in rodents is a commonly studied model of a compensatory increase in insulin secretion and β-cell mass; β-cells eventually fail, leading to glucose intolerance and insulin intolerance. The HFD model shows an initial increased expression of β-cell functional genes, which is followed by a cessation of gene hyperexpression, endoplasmic reticulum stress, and β-cell functional failure (24). We observed an increase in β-cell mass in the islets of control mice and at early ages in the islets of βVmat2KO mice. However, in βVmat2KO islets, both β-cell mass and insulin secretion were impaired with increasing age. β-cell failure corresponded with a decrease in β-cell mass. Decreased expression of maturation markers, such as *Ins1*, *Ins2*, *Glut2*, *Gck*, *Pdx1*, *Nkx6.1*, and *MafA*, and increased expression of the dedifferentiation marker *MafB* occur in islets of βVmat2KO mice, which is in parallel with β-cell failure and precedes the decrease in β-cell mass. Our results agree with previous reports that dedifferentiation is one of the mechanisms of β-cell failure.

### Dopamine Actions in Neuronal Cells

In neuronal cells, VMAT2 plays an important role in the compartmentation of dopamine to protect the cells from oxidative stress. Improper compartmentation of dopamine contributes to diseases in the neural system such as Parkinson disease. Accumulation of dopamine in the cytosolic space is toxic, inducing neuronal damage and apoptotic cell death (37–40). Dopamine can be auto-oxidized to form ROS, including hydroxyl radicals, superoxide, and hydrogen peroxide. Oxidized dopamine can then be converted to highly toxic dopamine quinones and the protein function-altering cysteinyl adduct. Deamination by mitochondrial MAO converts cytosolic dopamine to hydroxyperoxide and a reactive aldehyde intermediate, which can be oxidized to create ROS (41,42). Genetic knockout of *Vmat2* is reported to be lethal. Animals with *Vmat2* knockouts are hypersensitive to the dopamine agonist apomorphine, and the psychostimulants cocaine and amphetamine, with animals dying a few days after birth (4). Animals with very low VMAT2 levels were reported to survive into adulthood but were more vulnerable to neural damage in the dopaminergic neurons (37,43). On the other hand, increasing dopamine stores by overexpression of VMAT2 attenuated cytosolic dopamine levels and enhanced dopaminergic cell survival by lowering dopamine-dependent oxidative stress (3,44).

### Dopamine as a Negative Regulator for Insulin Secretion in Pancreatic β-Cells

In pancreatic β-cells, dopamine reportedly functions as a negative regulator for insulin secretion through Drd2. The knockdown of Drd2 in INS-1 cells (a β-cell line) resulted in increased insulin secretion (12). Dopamine treatment decreased insulin secretion in isolated islets (45). We previously reported that dopamine accelerated β-cell dedifferentiation, which could be rescued with the Drd2 antagonist domperidone (17). Long-term VMAT2 deficiency resulted in β-cell failure. This phenotype is in agreement with the previously reported mouse model with Drd2 disruption, which resulted in an impairment in glucose tolerance, diminished β-cell mass, and decreased β-cell replication (15). We interpret this to mean that loss of dopamine-negative signaling enhances insulin secretion. Insulin exocytosis accompanied dopamine exocytosis. Increased insulin secretion increases dopamine release extracellularly. Dopamine into the cytosol is degraded by MAO, which increases the ROS level, thereby contributing to β-cell dysfunction. Islet-specific MAO expression depends on the transcriptional activity of the mature endocrine β-cell marker MAFA. Therefore, mature β-cells develop a mechanism to degrade dopamine and increase the ROS level (16). Although βVmat2KO islets exhibit lower dopamine content compared with the control mice, a certain level of dopamine still exists, since the dopamine-synthesizing enzyme tyrosine hydroxylase is expressed in β-cells (46).

### Glucotoxicity and β-Cell Failure

Chronic exposure to high glucose causes functional damage to pancreatic β-cells, which is known as glucose toxicity. One mechanism of glucose toxicity is oxidative stress (47) conferred by ROS (1,48). Administration of an antioxidant such as glutathione ameliorates glucotoxicity (49). ROS generation through dopamine degradation seems to play an important role in glucotoxicity. Here, we showed that

an MAOB inhibitor, pargyline, reduced the level of ROS in βVmat2KO islets stimulated by glucose.

Chronic hyperglycemia models are reported to lead to β-cell dysfunction in the long-term. Inducible mouse models selectively expressing gain-of-function $K_{ATP}$ channel mutations (Kir6.2-V59M or K185QΔN30) in pancreatic β-cells show β-cell dysfunction due to β-cell dedifferentiation (50,51). Furthermore, loss-of-function mutants of the voltage-dependent K+ (Kv) channel KCNH6 plays a role in the modulation of insulin secretion. In a loss-of-function KCNH6 mutant in humans and mice, hyper–insulin secretion was observed initially, followed by subsequent hypo–insulin secretion as a result of overstimulation of insulin secretion; in the long-term, endoplasmic reticulum stress, apoptosis, loss of β-cell mass, and subsequent decreased insulin secretion were observed (52). These reports suggest that the overstimulation of insulin secretion causes β-cell failure in the long-term, which is in agreement with our results.

### VMAT2 as a Guardian for Maintenance of β-Cell Function

β-cells are highly heterogeneous (53–55), which protects β-cells themselves from overstimulation. Under normal conditions, β-cells secrete dopamine in response to high blood glucose. The secreted dopamine acts through Drd2 on their plasma membrane to negatively regulate insulin secretion. Dopamine is rapidly sequestered into the β-cells by DAT and stored in vesicles by VMAT2, thereby protecting β-cells from dopamine toxicity. However, miscompartmentalization of dopamine might occur with overstimulation of insulin secretion or low VMAT2 expression, increasing ROS accumulation and leading to β-cell failure. Future works on how the dopamine-VMAT2 signaling system works in the heterogenous β-cell population would be necessary to increase the understanding of VMAT2 in the maintenance of β-cell function.

**Acknowledgments.** The authors thank the members of the Animal Centers and the Bio Resource Department at the Tokyo Institute of Technology and Kumamoto University for technical assistance. The authors thank Takeshi Nagura (Kumamoto University) for discussions and technical assistance.

**Funding.** This work was supported by a grant from the Project for Realization of Regenerative Medicine from Japan Agency for Medical Research and Development (AMED) (grant number 17bm0704004h0101) and Grants-in-Aid from the Ministry of Education, Culture, Sports, Science and Technology, Japan (18H02861 to S.K. and 17K09455 to D.S.). This work was also supported in part by the Takeda Science Foundation and Japan Insulin Dependent Diabetes Mellitus (IDDM) Network.

**Duality of Interest.** No potential conflicts of interest relevant to this article were reported.

**Author Contributions.** D.S. designed the experiments and acquired, analyzed, and interpreted data. F.U., H.T., Y.S., and K.M. acquired and analyzed the data. N.T. performed blastocyst injection of the ES cells and generated the $Slc18a2^{tm1a/+}$ mouse. N.N. provided technical advice and support for the maintenance of gene knockout mice. K.K. and N.S. discussed the data. S.K. provided conceptual input, discussion, writing, and revision of the manuscript; approved the final version of the manuscript; and obtained funding. D.S. and S.K. are the guarantors of this work and, as such, had full access to all the data in the study and take responsibility for the integrity of the data and the accuracy of the data analysis.

### References

1. Gerber PA, Rutter GA. The role of oxidative stress and hypoxia in pancreatic beta-cell dysfunction in diabetes mellitus. Antioxid Redox Signal 2017;26:501–518

2. Newsholme P, Cruzat VF, Keane KN, Carlessi R, de Bittencourt PIH Jr. Molecular mechanisms of ROS production and oxidative stress in diabetes. Biochem J 2016;473:4527–4550

3. Vergo S, Johansen JL, Leist M, Lotharius J. Vesicular monoamine transporter 2 regulates the sensitivity of rat dopaminergic neurons to disturbed cytosolic dopamine levels. Brain Res 2007;1185:18–32

4. Wang YM, Gainetdinov RR, Fumagalli F, et al. Knockout of the vesicular monoamine transporter 2 gene results in neonatal death and supersensitivity to cocaine and amphetamine. Neuron 1997;19:1285–1296

5. Eiden LE, Weihe E. VMAT2: a dynamic regulator of brain monoaminergic neuronal function interacting with drugs of abuse. Ann N Y Acad Sci 2011;1216:86–98

6. Anlauf M, Eissele R, Schäfer MKH, et al. Expression of the two isoforms of the vesicular monoamine transporter (VMAT1 and VMAT2) in the endocrine pancreas and pancreatic endocrine tumors. J Histochem Cytochem 2003;51:1027–1040

7. Saisho Y, Harris PE, Butler AE, et al. Relationship between pancreatic vesicular monoamine transporter 2 (VMAT2) and insulin expression in human pancreas. J Mol Histol 2008;39:543–551

8. Schäfer MK-H, Hartwig NR, Kalmbach N, et al. Species-specific vesicular monoamine transporter 2 (VMAT2) expression in mammalian pancreatic beta cells: implications for optimising radioligand-based human beta cell mass (BCM) imaging in animal models. Diabetologia 2013;56:1047–1056

9. Harris PE, Ferrara C, Barba P, Polito T, Freeby M, Maffei A. VMAT2 gene expression and function as it applies to imaging beta-cell mass. J Mol Med (Berl) 2008;86:5–16

10. Simpson NR, Souza F, Witkowski P, et al. Visualizing pancreatic beta-cell mass with [$^{11}$C]DTBZ. Nucl Med Biol 2006;33:855–864

11. Sakano D, Shiraki N, Kikawa K, et al. VMAT2 identified as a regulator of late-stage β-cell differentiation. Nat Chem Biol 2014;10:141–148

12. Rubí B, Ljubicic S, Pournourmohammadi S, et al. Dopamine D2-like receptors are expressed in pancreatic beta cells and mediate inhibition of insulin secretion. J Biol Chem 2005;280:36824–36832

13. Raffo A, Hancock K, Polito T, et al. Role of vesicular monoamine transporter type 2 in rodent insulin secretion and glucose metabolism revealed by its specific antagonist tetrabenazine. J Endocrinol 2008;198:41–49

14. Ustione A, Piston DW. Dopamine synthesis and D3 receptor activation in pancreatic β-cells regulates insulin secretion and intracellular [Ca(2+)] oscillations. Mol Endocrinol 2012;26:1928–1940

15. García-Tornadú I, Ornstein AM, Chamson-Reig A, et al. Disruption of the dopamine d2 receptor impairs insulin secretion and causes glucose intolerance. Endocrinology 2010;151:1441–1450

16. Ganic E, Johansson JK, Bennet H, Fex M, Artner I. Islet-specific monoamine oxidase A and B expression depends on MafA transcriptional activity and is compromised in type 2 diabetes. Biochem Biophys Res Commun 2015;468:629–635

17. Sakano D, Choi S, Kataoka M, et al. Dopamine D2 receptor-mediated regulation of pancreatic β cell mass. Stem Cell Reports 2016;7:95–109

18. Doura T, Kamiya M, Obata F, et al. Detection of *LacZ*-positive cells in living tissue with single-cell resolution. Angew Chem Int Ed Engl 2016;55:9620–9624

19. Kikawa K, Sakano D, Shiraki N, et al. Beneficial effect of insulin treatment on islet transplantation outcomes in Akita mice. PLoS One 2014;9:e95451

20. Freeby M, Ichise M, Harris PE. Vesicular monoamine transporter, type 2 (VMAT2) expression as it compares to insulin and pancreatic polypeptide in the head, body and tail of the human pancreas. Islets 2012;4:393–397

21. Gannon M, Shiota C, Postic C, Wright CVE, Magnuson M. Analysis of the Cre-mediated recombination driven by rat insulin promoter in embryonic and adult mouse pancreas. Genesis 2000;26:139–142
22. Lee JY, Ristow M, Lin X, White MF, Magnuson MA, Hennighausen L. RIP-Cre revisited, evidence for impairments of pancreatic β-cell function. J Biol Chem 2006;281:2649–2653
23. Navarro G, Abdolazimi Y, Zhao Z, et al. Genetic disruption of adenosine kinase in mouse pancreatic β-cells protects against high-fat diet-induced glucose intolerance. Diabetes 2017;66:1928–1938
24. Gupta D, Jetton TL, LaRock K, et al. Temporal characterization of β cell-adaptive and -maladaptive mechanisms during chronic high-fat feeding in C57BL/6NTac mice. J Biol Chem 2017;292:12449–12459
25. Talchai C, Xuan S, Lin HV, Sussel L, Accili D. Pancreatic β cell dedifferentiation as a mechanism of diabetic β cell failure. Cell 2012;150:1223–1234
26. Md Moin AS, Dhawan S, Shieh C, Butler PC, Cory M, Butler AE. Increased hormone-negative endocrine cells in the pancreas in type 1 diabetes. J Clin Endocrinol Metab 2016;101:3487–3496
27. Doussau F, Augustine GJ. The actin cytoskeleton and neurotransmitter release: an overview. Biochimie 2000;82:353–363
28. Stamateris RE, Sharma RB, Hollern DA, Alonso LC. Adaptive β-cell proliferation increases early in high-fat feeding in mice, concurrent with metabolic changes, with induction of islet cyclin D2 expression. Am J Physiol Endocrinol Metab 2013;305:E149–E159
29. Tersey SA, Levasseur EM, Syed F, et al. Episodic β-cell death and dedifferentiation during diet-induced obesity and dysglycemia in male mice. FASEB J 2018;32:6150–6158
30. Pizzinat N, Copin N, Vindis C, Parini A, Cambon C. Reactive oxygen species production by monoamine oxidases in intact cells. Naunyn Schmiedebergs Arch Pharmacol 1999;359:428–431
31. Sampson SR, Bucris E, Horovitz-Fried M, et al. Insulin increases H2O2-induced pancreatic beta cell death. Apoptosis 2010;15:1165–1176
32. Robertson RP. Chronic oxidative stress as a central mechanism for glucose toxicity in pancreatic islet beta cells in diabetes. J Biol Chem 2004;279:42351–42354
33. Llanos P, Contreras-Ferrat A, Barrientos G, Valencia M, Mears D, Hidalgo C. Glucose-dependent insulin secretion in pancreatic β-cell islets from male rats requires $Ca^{2+}$ release via ROS-stimulated ryanodine receptors. PLoS One 2015;10:e0129238
34. Tummala KS, Kottakis F, Bardeesy N. NRF2: translating the redox code. Trends Mol Med 2016;22:829–831
35. Schultheis J, Beckmann D, Mulac D, Müller L, Esselen M, Düfer M Nrf2 activation protects mouse beta cells from glucolipotoxicity by restoring mitochondrial function and physiological redox balance. Oxid Med Cell Longev. 2019;2019:7518510
36. Borelli MI, Rubio M, García ME, Flores LE, Gagliardino JJ. Tyrosine hydroxylase activity in the endocrine pancreas: changes induced by short-term dietary manipulation. BMC Endocr Disord 2003;3:2
37. Caudle WM, Richardson JR, Wang MZ, et al. Reduced vesicular storage of dopamine causes progressive nigrostriatal neurodegeneration. J Neurosci 2007;27:8138–8148
38. Lohr KM, Stout KA, Dunn AR, et al. Increased vesicular monoamine transporter 2 (VMAT2; Slc18a2) protects against methamphetamine toxicity. ACS Chem Neurosci 2015;6:790–799
39. Masoud ST, Vecchio LM, Bergeron Y, et al. Increased expression of the dopamine transporter leads to loss of dopamine neurons, oxidative stress and l-DOPA reversible motor deficits. Neurobiol Dis 2015;74:66–75
40. Uhl GR. Dopamine compartmentalization, selective dopaminergic vulnerabilities in Parkinson's disease and therapeutic opportunities. Ann Clin Transl Neurol 2019;6:406–415
41. Eisenhofer G, Kopin IJ, Goldstein DS. Catecholamine metabolism: a contemporary view with implications for physiology and medicine. Pharmacol Rev 2004;56:331–349
42. Goldstein DS, Sullivan P, Holmes C, et al. Determinants of buildup of the toxic dopamine metabolite DOPAL in Parkinson's disease. J Neurochem 2013;126:591–603
43. Mooslehner KA, Chan PM, Xu W, et al. Mice with very low expression of the vesicular monoamine transporter 2 gene survive into adulthood: potential mouse model for parkinsonism. Mol Cell Biol 2001;21:5321–5331
44. Lohr KM, Chen M, Hoffman CA, et al. Vesicular monoamine transporter 2 (VMAT2) level regulates MPTP vulnerability and clearance of excess dopamine in mouse striatal terminals. Toxicol Sci 2016;153:79–88
45. Garcia Barrado MJ, Iglesias Osma MC, Blanco EJ, et al. Dopamine modulates insulin release and is involved in the survival of rat pancreatic beta cells. PLoS One 2015;10:e0123197
46. Vázquez P, Robles AM, de Pablo F, Hernández-Sánchez C. Non-neural tyrosine hydroxylase, via modulation of endocrine pancreatic precursors, is required for normal development of beta cells in the mouse pancreas. Diabetologia 2014;57:2339–2347
47. Robertson RP, Tanaka Y, Takahashi H, Tran POT, Harmon JS. Prevention of oxidative stress by adenoviral overexpression of glutathione-related enzymes in pancreatic islets. Ann N Y Acad Sci 2005;1043:513–520
48. Pullen TJ, Rutter GA. When less is more: the forbidden fruits of gene repression in the adult β-cell. Diabetes Obes Metab 2013;15:503–512
49. Zhang J, An H, Ni K, et al. Glutathione prevents chronic oscillating glucose intake-induced β-cell dedifferentiation and failure. Cell Death Dis 2019;10:321
50. Wang Z, York NW, Nichols CG, Remedi MS. Pancreatic β cell dedifferentiation in diabetes and redifferentiation following insulin therapy. Cell Metab 2014;19:872–882
51. Brereton MF, Iberl M, Shimomura K, et al. Reversible changes in pancreatic islet structure and function produced by elevated blood glucose. Nat Commun 2014;5:4639
52. Yang JK, Lu J, Yuan SS, et al. From hyper- to hypoinsulinemia and diabetes: effect of KCNH6 on insulin secretion. Cell Rep 2018;25:3800–3810.e6
53. Bader E, Migliorini A, Gegg M, et al. Identification of proliferative and mature β-cells in the islets of Langerhans. Nature 2016;535:430–434
54. Dorrell C, Schug J, Canaday PS, et al. Human islets contain four distinct subtypes of β cells. Nat Commun 2016;7:11756
55. Tritschler S, Theis FJ, Lickert H, Böttcher A. Systematic single-cell analysis provides new insights into heterogeneity and plasticity of the pancreas. Mol Metab 2017;6:974–990